

Exclusive coherent production of heavy vector mesons in nucleus-nucleus collisions at LHC

A. Cisek,^{1,*} W. Schäfer,^{1,†} and A. Szczurek^{1,2,‡}

¹*Institute of Nuclear Physics PAN, PL-31-342 Kraków, Poland*

²*Institute of Physics, University of Rzeszów, Poland*

(Dated: November 18, 2018)

Abstract

Heavy nuclei at collider energies are a source of high energy Weizsäcker-Williams photons. This photon flux may be utilized to study high energy photon-nucleus interactions. Here we concentrate on the coherent diffractive production of heavy vector mesons on nuclear targets and show how it probes the unintegrated glue of the nucleus in the saturation domain. We present predictions for rapidity distributions of exclusive coherent J/Ψ and Υ mesons which can be measured by the ALICE experiment at the LHC.

PACS numbers: 13.87.-a, 11.80La, 12.38.Bx, 13.85.-t

arXiv:1204.5381v1 [hep-ph] 24 Apr 2012

*Electronic address: Anna.Cisek@ifj.edu.pl

†Electronic address: Wolfgang.Schafer@ifj.edu.pl

‡Electronic address: Antoni.Szczurek@ifj.edu.pl

I. INTRODUCTION

The exclusive photo- and electroproduction of vector mesons at high energies has recently been thoroughly studied at the electron–proton collider HERA (for a review, see [1]). In a Regge picture, this process is driven by a t -channel Pomeron exchange. The HERA data, which range from low to high photon virtuality as well as from light to heavy vector mesons, have given an intriguing insight into the Pomeron physics from soft to hard processes. Overall a consistent phenomenology emerges, in which the QCD-Pomeron exchange is modelled by the gluon-ladder exchange and quantified by the unintegrated gluon distribution of the target proton or the color dipole-proton cross section.

In recent years, the very-small x behaviour of the gluon structure function has been of great interest in the context of unitarity effects and the saturation phenomena [2].

The multiple scattering/absorption effects associated with the gluon saturation physics are naturally enhanced on a large nuclear target. From this point of view the coherent diffractive production of vector mesons on heavy nuclei is very interesting. Clearly, the best option to study the small- x nuclear glue would be a dedicated electron-ion collider [3], where for example one could measure nuclear structure functions at perturbatively large Q^2 . Lacking such a facility, there appears to be no easy experimental access to the nuclear gluon distribution.

Here, the exclusive photoproduction of heavy vector mesons J/Ψ , Υ opens up a new possibility to experimentally study the small- x nuclear glue. It is the large mass of the heavy quark which provides the hard scale and assures that we may use perturbation theory even in the photoproduction limit.

Presently, nucleus-nucleus collisions at $\sqrt{s_{NN}} = 2.76$ TeV studied at the LHC offer an access to high-energy photonuclear reactions [4]. Here, one of the nuclei will serve as a source of Weizsäcker-Williams photons, while the other one plays the role of a target. Coherent diffractive processes of interest in this work leave the target intact and deflected only by a very small angle. Diffractive photoproduction of light vector mesons on nuclei is an old subject [5], and with some success can be addressed using vector-meson dominance, and within a limited range of energies, a hadronic Glauber coupled channel type of model. When a hard scale is present - such as a large photon virtuality,

or a large quark mass - it proves more efficient to use perturbative QCD degrees of freedom. In particular the color-dipole formulation to which we will now turn allows to account for nuclear effects in a rather straightforward manner.

II. AMPLITUDE AND CROSS SECTION FOR $\gamma A \rightarrow VA$ REACTION

A. Vector meson production in the color-dipole picture

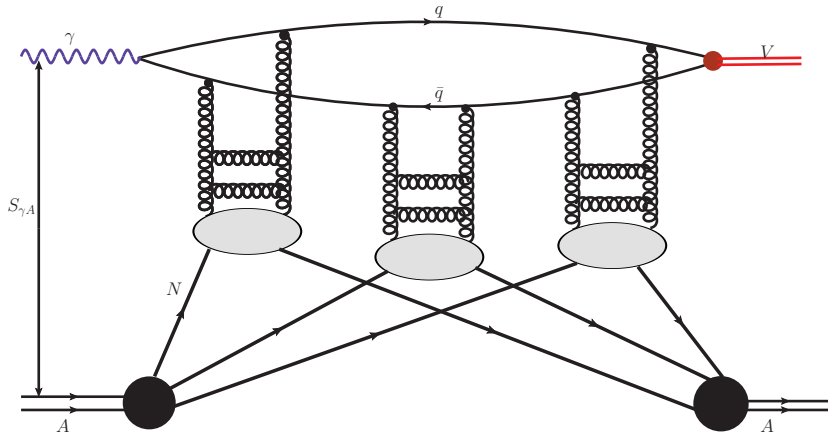


FIG. 1: Sample diagram for the $\gamma A \rightarrow VA$ amplitude. At $x \sim x_A$ the relevant degree of freedom is the $Q\bar{Q}$ dipole. All multipomeron exchange diagrams are summed up by the Glauber-Gribov multiple scattering theory for color dipoles.

It is useful to start from the color-dipole formulation [6] of vector meson photoproduction. This formulation is essentially equivalent to the k_{\perp} -factorization approach which we previously used for the free proton target [7], and to which we turn later in this work. The multiple scattering corrections relevant for nuclear targets are however more easily derived in impact parameter space.

The forward amplitude for vector-meson photoproduction on the nuclear target at center-of mass energy W ($x = m_V^2/W^2$), takes the form

$$A(\gamma A \rightarrow Vp; W) = i \langle V | \sigma_A(x, \mathbf{r}) | \gamma \rangle = 2i \int d^2\mathbf{b} \langle V | \Gamma_A(x, \mathbf{b}, \mathbf{r}) | \gamma \rangle$$

$$= 2i \int d^2\mathbf{b} \int_0^1 dz \int d^2\mathbf{r} \psi_V^*(z, \mathbf{r}) \psi_\gamma(z, \mathbf{r}) \Gamma_A(x, \mathbf{b}, \mathbf{r}). \quad (1)$$

Here $\psi_V(z, \mathbf{r}), \psi_\gamma(x, \mathbf{r})$ are the light-cone wave-functions of the vector meson and the photon, respectively. For simplicity we suppress the summation over (anti-)quark helicities. The explicit form of the wave function are not important for the argument in this section, we will later give all explicit formulas in momentum space.

The amplitude can be easily generalized to finite transverse momentum transfer Δ :

$$A(\gamma A \rightarrow Vp; W, \Delta) = 2i \int d^2\mathbf{b} \exp[-i\mathbf{b}\Delta] \langle V | \Gamma_A(x, \mathbf{b}, \mathbf{r}) | \gamma \rangle. \quad (2)$$

The differential cross section is then given by ($t = -\Delta^2$):

$$\frac{d\sigma(\gamma A \rightarrow VA; W)}{dt} = \frac{d\sigma(\gamma A \rightarrow VA; W)}{d\Delta^2} = \frac{1}{16\pi} |A(\gamma A \rightarrow Vp; W, \Delta)|^2. \quad (3)$$

Following [8], at small x ($x \lesssim x_A = 0.1A^{-1/3}$), the multiple scatterings of the color-dipole can be summed up by a Glauber-series for color dipoles. The color-dipole-nucleus amplitude in impact parameter space for $x \sim x_A$ can then be given in terms of the color-dipole-proton cross section:

$$\Gamma_A(x_A, \mathbf{b}, \mathbf{r}) = 1 - \exp\left(-\frac{1}{2}\sigma(x_A, \mathbf{r})T_A(\mathbf{b})\right). \quad (4)$$

In practice that means $x_A \sim 0.01$. For smaller x one must take into account higher, $q\bar{q}g$ -Fock states as we discuss below.

In order to quantify the size of nuclear (multiple scattering) effects, one often compares to the impulse approximation. The latter works well if multiple scatterings are weak, i.e. if the nuclear opacity $\sigma(x_A, \mathbf{r})T_A(\mathbf{b})/2$ is small. In impulse approximation we assume that only one of the nucleons in the nucleus participates in the interaction, and all others are spectators. Expanding the Glauber-exponential to the first order we obtain (hereafter IA stands for impulse approximation):

$$A_{\text{IA}}(\gamma A \rightarrow VA; W, \Delta) = i \langle V | \sigma(x, \mathbf{r}) | \gamma \rangle \int d^2\mathbf{b} \exp[-i\mathbf{b}\Delta] T_A(\mathbf{b}). \quad (5)$$

The total cross section in impulse approximation would then be

$$\sigma_{\text{tot;IA}}(\gamma A \rightarrow VA; W) = 4\pi \frac{d\sigma(\gamma p \rightarrow Vp)}{dt} \Big|_{t=0} \int d^2\mathbf{b} T_A^2(\mathbf{b}). \quad (6)$$

Let us introduce the ratio of the full nuclear cross section to the impulse approximation result:

$$R_{\text{coh}}(W) = \frac{\sigma_{\text{tot}}(\gamma A \rightarrow VA; W)}{\sigma_{\text{tot,IA}}(\gamma A \rightarrow VA; W)}. \quad (7)$$

Then we can also express the total photoproduction cross section on the nucleus as:

$$\sigma_{\text{tot}}(\gamma A \rightarrow VA; W) = R_{\text{coh}}(W) \cdot 4\pi \frac{d\sigma(\gamma p \rightarrow Vp)}{dt} \Big|_{t=0} \int d^2\mathbf{b} T_A^2(\mathbf{b}). \quad (8)$$

Here

$$\frac{d\sigma(\gamma p \rightarrow Vp)}{dt} \Big|_{t=0} \approx B_V \cdot \sigma_{\text{tot}}(\gamma p \rightarrow Vp), \quad (9)$$

where B_V is the diffraction slope, can be taken from experimental data [9–11].

The integral over the nuclear optical density squared behaves parametrically as (see e.g. [12]):

$$\int d^2\mathbf{b} T_A^2(\mathbf{b}) = C_A \cdot \frac{3A^2}{4\pi R_{\text{ch}}^2}, \quad (10)$$

where R_{ch} is the nuclear charge radius, and C_A is a number of order unity which depends on the shape of $T_A(\mathbf{b})$. In the numerical calculations, we use a realistic nuclear density, as parametrized in [13].

B. Momentum space formulation of vector-meson production on nuclei

We can bring the photoproduction amplitude for the nuclear target into the similar k_{\perp} -factorization form as the result for the free proton. The only difference is that now the unintegrated gluon distribution of the proton, will be replaced by the appropriately defined unintegrated glue of the nucleus, explicitly constructed in the treatment of the diffractive $\pi A \rightarrow q\bar{q}A$ process in [12].

Recall now, that for the free-nucleon target, dipole cross section and unintegrated gluon distribution are related by [14]

$$\sigma(x, \mathbf{r}) = \sigma_0 \int d^2\boldsymbol{\kappa} [1 - e^{i\boldsymbol{\kappa}\mathbf{r}}] \alpha_S f(x, \boldsymbol{\kappa}), \quad (11)$$

where we pulled out $\sigma_0 = \sigma_0(x)$, so that f is normalized to unity:

$$f(x, \boldsymbol{\kappa}) = \frac{1}{\sigma_0} \frac{4\pi}{N_c} \frac{1}{\boldsymbol{\kappa}^4} \frac{\partial G_N(x, \boldsymbol{\kappa}^2)}{\partial \log(\boldsymbol{\kappa}^2)}, \quad \sigma_0(x) = \int d^2\boldsymbol{\kappa} \frac{4\pi}{N_c} \frac{1}{\boldsymbol{\kappa}^4} \frac{\partial G_N(x, \boldsymbol{\kappa}^2)}{\partial \log(\boldsymbol{\kappa}^2)}. \quad (12)$$

We can analogously introduce the impact-parameter dependent unintegrated gluon distribution of the nucleus $\phi(\mathbf{b}, x, \boldsymbol{\kappa})$ through the relation

$$\Gamma_A(x, \mathbf{b}, \boldsymbol{r}) = \int d^2\boldsymbol{\kappa} [1 - e^{i\boldsymbol{\kappa}\boldsymbol{r}}] \phi(\mathbf{b}, x, \boldsymbol{\kappa}). \quad (13)$$

In terms of the nuclear glue G_A , the function $\phi(\mathbf{b}, x, \boldsymbol{\kappa})$ fulfills

$$\phi(\mathbf{b}, x, \boldsymbol{\kappa}) = \frac{2\pi\alpha_S(\boldsymbol{\kappa})}{N_c} \frac{1}{\boldsymbol{\kappa}^4} \frac{\partial G_A(\mathbf{b}, x, \boldsymbol{\kappa}^2)}{\partial \log \boldsymbol{\kappa}^2 d^2\mathbf{b}}. \quad (14)$$

In the forward scattering limit, i.e. for $\boldsymbol{\Delta} = 0$ the photoproduction amplitude given in [1] can be brought in the form (see [7]):

$$\begin{aligned} \Im m \mathcal{T}(W, \Delta^2 = 0) &= W^2 \frac{c_v \sqrt{4\pi\alpha_{em}}}{4\pi^2} 2 \int_0^1 \frac{dz}{z(1-z)} \int_0^\infty \pi dk^2 \psi_V(z, k^2) \\ &\int_0^\infty \frac{\pi dk^2}{\boldsymbol{\kappa}^4} \alpha_S(q^2) \mathcal{F}_A(x, \boldsymbol{\kappa}^2) \left(A_0(z, k^2) W_0(k^2, \boldsymbol{\kappa}^2) + A_1(z, k^2) W_1(k^2, \boldsymbol{\kappa}^2) \right), \end{aligned} \quad (15)$$

where

$$A_0(z, k^2) = m_Q^2 + \frac{k^2 m_Q}{M + 2m_Q}, \quad (16)$$

$$A_1(z, k^2) = \left[z^2 + (1-z)^2 - (2z-1)^2 \frac{m_Q}{M + 2m_Q} \right] \frac{k^2}{k^2 + m_Q^2}, \quad (17)$$

$$W_0(k^2, \boldsymbol{\kappa}^2) = \frac{1}{k^2 + m_Q^2} - \frac{1}{\sqrt{(k^2 - m_Q^2 - \boldsymbol{\kappa}^2)^2 + 4m_Q^2 k^2}}, \quad (18)$$

$$W_1(k^2, \boldsymbol{\kappa}^2) = 1 - \frac{k^2 + m_Q^2}{2k^2} \left(1 + \frac{k^2 - m_Q^2 - \boldsymbol{\kappa}^2}{\sqrt{(k^2 - m_Q^2 - \boldsymbol{\kappa}^2)^2 + 4m_Q^2 k^2}} \right). \quad (19)$$

Here m_Q is the heavy quark mass, and

$$M^2 = \frac{k^2 + m_Q^2}{z(1-z)} \quad (20)$$

is the invariant mass squared of the $Q\bar{Q}$ system in the final state. The strong coupling enters at the hard scale $q^2 = \max(\boldsymbol{\kappa}^2, k^2 + m_Q^2)$. The light-cone wave function ψ_V of the vector meson is parametrised exactly as in [1, 7], and the Gaussian form, which proved to lead to good agreement with experiment, is adopted.

All nuclear effects are accounted for by the substitution

$$\frac{\alpha_S}{\boldsymbol{\kappa}^4} \mathcal{F}_A(x, \boldsymbol{\kappa}^2) = \int d^2\mathbf{b} \frac{\alpha_S}{\boldsymbol{\kappa}^4} \frac{\partial G_A(\mathbf{b}, x, \boldsymbol{\kappa}^2)}{\partial \log \boldsymbol{\kappa}^2 d^2\mathbf{b}} = \frac{N_c}{2\pi} \int d^2\mathbf{b} \phi(\mathbf{b}, x, \boldsymbol{\kappa}). \quad (21)$$

In this way we introduce also the impact-parameter dependent amplitude by the relation

$$\Im \mathcal{T}(\gamma A \rightarrow VA) = \int d^2\mathbf{b} \Im \mathcal{T}(\gamma A \rightarrow VA; \mathbf{b}). \quad (22)$$

Its normalization is such that

$$\frac{d\sigma(\gamma A \rightarrow VA; W)}{d^2\mathbf{b}} = \frac{1}{4} \left| \frac{\Im \mathcal{T}(\gamma A \rightarrow VA; \mathbf{b})}{W^2} \right|^2. \quad (23)$$

C. The nuclear unintegrated glue in the Glauber regime

Here we briefly recapitulate how to calculate the nuclear unintegrated gluon distribution from the proton unintegrated glue.

The starting point is the definition of the nuclear unintegrated glue (13). We are interested in the regime of $x \sim x_A$, where the Glauber representation of the color-dipole scattering amplitude $\Gamma(x, \mathbf{b}, \mathbf{r})$ is valid:

$$\Gamma(x_A, \mathbf{b}, \mathbf{r}) = 1 - \exp\left[\frac{1}{2}\sigma(x_A, \mathbf{r})T_A(\mathbf{b})\right]. \quad (24)$$

Introducing the shorthand notation

$$\nu(\mathbf{b}) = \frac{1}{2} \alpha_S \sigma_0(x_A) T_A(\mathbf{b}), \quad (25)$$

and the multiple convolutions

$$f^{(j)}(x, \boldsymbol{\kappa}) = \int d^2\boldsymbol{\kappa}_1 \dots d^2\boldsymbol{\kappa}_j \delta^{(2)}(\boldsymbol{\kappa} - \sum_i \boldsymbol{\kappa}_i) f(x, \boldsymbol{\kappa}_1) \dots f(x, \boldsymbol{\kappa}_j), f^{(0)}(\boldsymbol{\kappa}) \equiv \delta^{(2)}(\boldsymbol{\kappa}), \quad (26)$$

we obtain the expansion of the Glauber exponential

$$\exp\left[-\frac{1}{2}\sigma(x_A, \mathbf{r})T_A(\mathbf{b})\right] = \sum_{k \geq 0} \int d^2\boldsymbol{\kappa} \exp[i\boldsymbol{\kappa}\mathbf{r}] w_k(\mathbf{b}) f^{(k)}(x_A, \boldsymbol{\kappa}) \quad (27)$$

with the Poisson-weights

$$w_k(\mathbf{b}) = \exp[-\nu(\mathbf{b})] \frac{\nu^k(\mathbf{b})}{k!}. \quad (28)$$

This gives us the expression of the nuclear unintegrated gluon distribution as an expansion over multiple convolutions of the free nucleon glue:

$$\phi(\mathbf{b}, x, \boldsymbol{\kappa}) = \sum_{j \geq 1} w_j(\mathbf{b}) f^{(j)}(x, \boldsymbol{\kappa}). \quad (29)$$

here, the j -th term of the expansion is the contribution of the interaction of j nucleons with the color dipole. Here $f^{(j)}(x, \boldsymbol{\kappa})$ is the collective unintegrated glue of j nucleons, and the weight factor w_j gives us the probability the j nucleons overlapping at impact parameter \mathbf{b} take part in the interaction.

It is important to realize that the nuclear unintegrated glue includes the multiple scattering corrections, it is not simply a two-gluon exchange in the crossed channel, as in the free nucleon glue. To some degree however, these multiple gluon exchanges behave like a two-gluon exchange: the diffractive amplitude has the same form as the two-gluon exchange amplitude on the free nucleon target.

D. Small- x -evolution: contribution of the $Q\bar{Q}g$ -Fock state

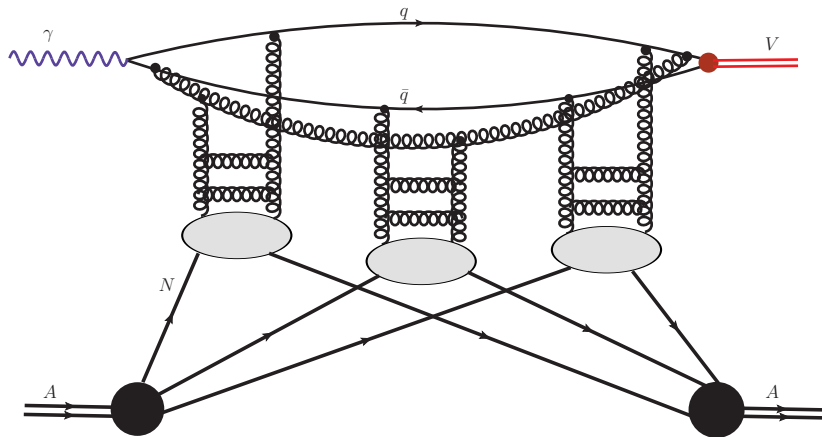


FIG. 2: A sample diagram which contains the multiple scattering of a $Q\bar{Q}g$ -Fock state. This is the first step in the nonlinear evolution of the nuclear unintegrated glue.

If we increase the γA center-of-mass energy successively higher and higher $Q\bar{Q}g, Q\bar{Q}gg, \dots$ Fock-states become important. On the free nucleon target, the effect of higher Fock-states, which contain gluons strongly ordered in rapidity can be resummed, and leads to the small- x evolution of the then x -dependent dipole cross section [14]. The multiple scatterings of the $Q\bar{Q}g$ -Fock state off a heavy nucleus are given by the first

iteration of the nonlinear Balitsky-Kovchegov [15] evolution equation

$$\frac{\partial\phi(\mathbf{b}, x, \mathbf{p})}{\partial\log(1/x)} = \mathcal{K}_{BFKL} \otimes \phi(\mathbf{b}, x, \mathbf{p}) + \mathcal{Q}[\phi](\mathbf{b}, x, \mathbf{p}).$$

The nuclear glue, which includes rescattering corrections of $Q\bar{Q}$ as well as $Q\bar{Q}g$ Fock states is then given by

$$\phi(\mathbf{b}, x, \mathbf{p}) = \phi(\mathbf{b}, x_A, \mathbf{p}) + \log\left(\frac{x_A}{x}\right) \cdot \frac{\partial\phi(\mathbf{b}, x, \mathbf{p})}{\partial\log(1/x)}. \quad (30)$$

In a similar manner, to obtain the ratio R_{coh} of eq.(7), the impulse approximation amplitude is calculated from

$$\phi_{\text{IA}}(\mathbf{b}, x_A, \mathbf{p}) = T_A(\mathbf{b}) \cdot \frac{4\pi\alpha_S}{N_c} \frac{1}{\kappa^4} \frac{\partial G_N(x, \kappa^2)}{\partial\log(\kappa^2)}, \quad (31)$$

subject to a similar iteration (30) as the full glue, but with the nonlinear piece omitted. For the explicit momentum-space form of the infrared-regularized BK-equation, see [16]. A similar strategy of including the $Q\bar{Q}$ and $Q\bar{Q}g$ -Fock states has been followed for the nuclear structure function and inclusive coherent diffraction in Ref.[17]. There a good agreement with available data on nuclear shadowing has been obtained. In the numerical calculations, we use an unintegrated gluon distribution of the proton that has been obtained from an analysis of HERA structure function data in [18].

Let us briefly discuss, how our approach differs from others available in the literature. The first estimates of Klein and Nystrand [19] are based on extracting an effective J/Ψ -nucleon cross section from photoproduction data using vector-meson dominance ideas. They then go on to use this cross section to evaluate the classical survival probability of mesons passing through a slab of nuclear matter. Goncalves and Machado [20] adopt the color dipole approach and give a proper quantum mechanical treatment of the multiple scattering effects. Their approach differs from ours in that they absorb all saturation effects into the dipole-nucleon cross section which is then eikonalized. This is strictly speaking inconsistent with the nonlinear evolution of the dipole-nucleus cross section, and neglects the fact that multiple scatterings off different nucleons are enhanced by the nuclear size. Of course it may well be viable phenomenologically in a limited range of energies. Finally, Rebyakova et al. [21] use a relation of the diffractive amplitude to the integrated gluon distribution of the target, which holds, with some reservations,

for heavy quarks. Such an approximation can be obtained from the k_{\perp} -factorization formalism used in this work to the leading logarithm in the hard scale (see [1] and references therein). There appears to be a hidden assumption that all saturation effects are summed up in a boundary condition of the integrated, collinear, nuclear glue.

III. RESULTS AND CONCLUSIONS

A. Photoproduction on nuclei: $\gamma A \rightarrow VA$

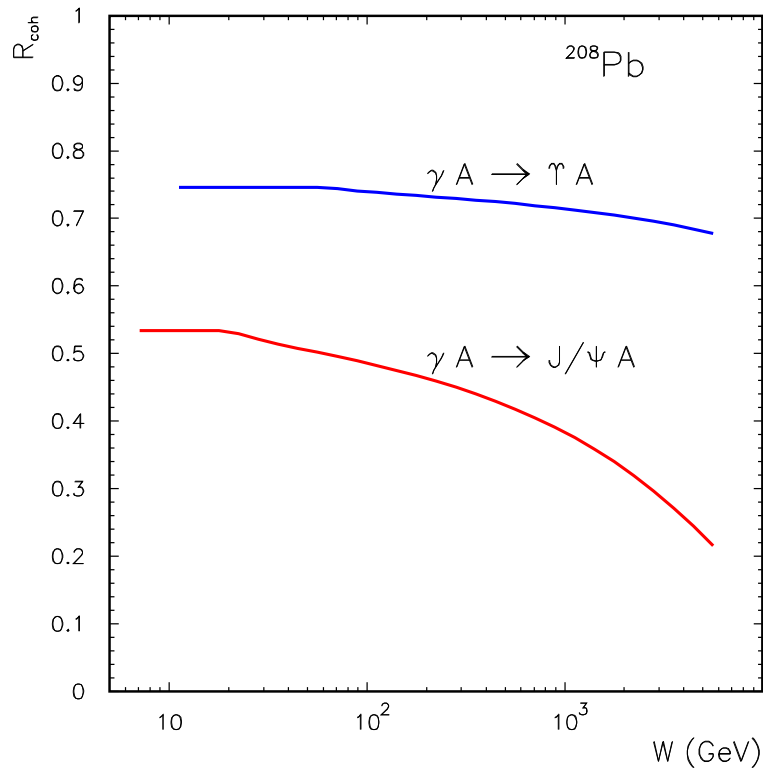


FIG. 3: Ratio of the nuclear coherent cross section for J/Ψ and Υ production to the Impulse Approximation cross section.

In Fig.3 we show the ratio $R_{coh}(W)$ for the lead nucleus (^{208}Pb) for J/Ψ (red line) and Υ (blue line) meson production. The deviation of R_{coh} from unity is a measure of the strength of nuclear rescattering/absorption effects. We see that the nuclear effects

are stronger for the J/Ψ than for the Υ meson. This is indeed to be expected, as we can most easily see in the dipole picture: the photoproduction amplitude probes the dipole cross section at the scanning radius $r_S \propto 1/m_Q$ [6], and the smaller dipoles relevant for Υ -production will experience smaller rescattering effects.

In Fig.4 we present the impact parameter distribution of vector meson photoproduction. We show results for J/Ψ and Υ mesons, for two different energies ($W = 200$, $W = 2760$ GeV) and lead nuclei.

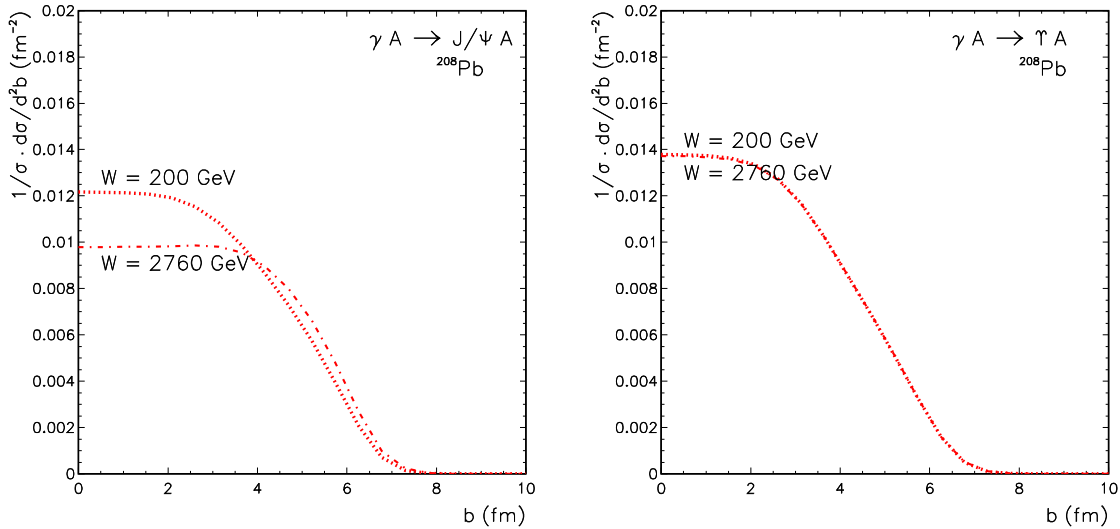


FIG. 4: Impact parameter distributions for J/Ψ and Υ mesons for the ^{208}Pb target.

B. Ultraperipheral nucleus-nucleus collisions: $AA \rightarrow AAV$

In the $AA \rightarrow AAV$ processes the heavy nuclei play two different roles. One of the nuclei is a target and the next is a source of high energy Weizäcker-Wiliams photons. In Fig.(5) we show Feynman diagrams for the relevant production mechanism, the Born diagram in the left panel and a diagram including the absorptive correction in the right panel. It should be noted that one should also add the amplitude in which the photon is emitted from the lower line. The interference of the photon emission from the upper or lower lines in fact causes a peculiar azimuthal correlation between the outgoing nuclei

[22]. After integration over azimuthal angles, and at the Born level, the interference drops out and we can add the squares of both amplitudes. If absorptive corrections are included, a small interference contribution remains even after azimuthal averaging [22]. Below we will neglect the interference effect and evaluate the nucleus-level cross section from the absorption corrected equivalent photon approximation:

$$\sigma(A_1 A_2 \rightarrow A_1 A_2 V; s) = \int d\omega \frac{dN_{A_1}^{\text{eff}}(\omega)}{d\omega} \sigma(\gamma A_2 \rightarrow V A_2; 2\omega\sqrt{s}) + (1 \leftrightarrow 2). \quad (32)$$

To obtain the effective photon flux dN^{eff} , one starts from the electric field strength associated with the moving nucleus (see for example Ref.[4] for a review and references) :

$$\mathbf{E}(\omega, \mathbf{b}) = Z\sqrt{4\pi\alpha_{em}} \int \frac{d^2\mathbf{q}}{(2\pi)^2} \exp[-i\mathbf{b}\mathbf{q}] \frac{\mathbf{q}F_{em}(\mathbf{q}^2 + \omega^2/\gamma^2)}{\mathbf{q}^2 + \omega^2/\gamma^2}. \quad (33)$$

Here $F_{em}(Q^2)$ is the charge form factor of the nucleus, ω is the photon energy, γ the relativistic Lorentz-boost of the beam and \mathbf{b} is the impact parameter. Having the electric

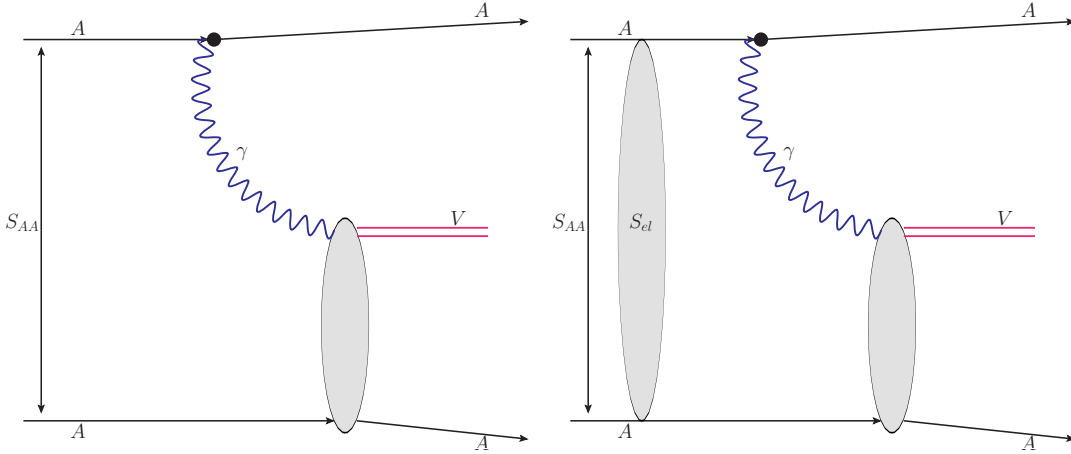


FIG. 5: Mechanism of exclusive vector-meson production in AA collisions. Left panel: Born diagram; Right panel: the elastic rescattering in the initial state accounts for the unitarity effect of inelastic channels.

field strength as a function of photon energy and impact parameter we can calculate the photon flux corresponding to the Born diagram in the left panel of Fig. 5:

$$dN(\omega, \mathbf{b}) = \frac{d\omega}{\omega} \frac{d^2\mathbf{b}}{\pi} |\mathbf{E}(\omega, \mathbf{b})|^2. \quad (34)$$

Finally, the effective photon flux with absorptive corrections included is:

$$dN^{eff}(\omega) = \int d^2\mathbf{b} S_{el}^2(\mathbf{b}) dN(\omega, \mathbf{b}).$$

The absorptive correction $S_{el}^2(\mathbf{b})$ is shown schematically by the extra oval in the right panel of Fig. 5. These absorptive correction can be calculated by applying the following simple formula (see e.g. [23]):

$$S_{el}^2(\mathbf{b}) = \exp\left(-\sigma_{NN} T_{A_1 A_2}(\mathbf{b})\right) \sim \theta(|\mathbf{b}| - (R_1 + R_2)), \quad (35)$$

where R_1 and R_2 are the radii of the colliding nuclei. We remove those configurations in the impact parameter space, when the nuclei overlap, which at high energy means automatically their break up. Therefore absorptive corrections have a meaning of the gap survival probability. In Fig. 6 we present the total cross section for J/Ψ and Υ

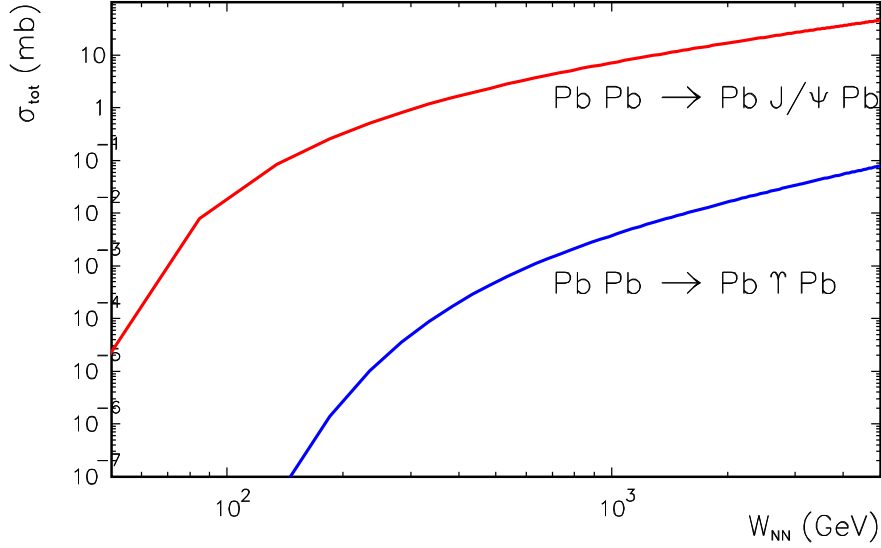


FIG. 6: Total cross section for $Pb Pb \rightarrow Pb J/\Psi Pb$ and $Pb Pb \rightarrow Pb \Upsilon Pb$ as a function of nucleon-nucleon energy.

production in nucleus-nucleus collisions as a function of energy for the ^{208}Pb target. The cross section for J/Ψ production increases by two-orders of magnitude when going from RHIC to LHC energy. For the Υ meson the corresponding increase of the cross section

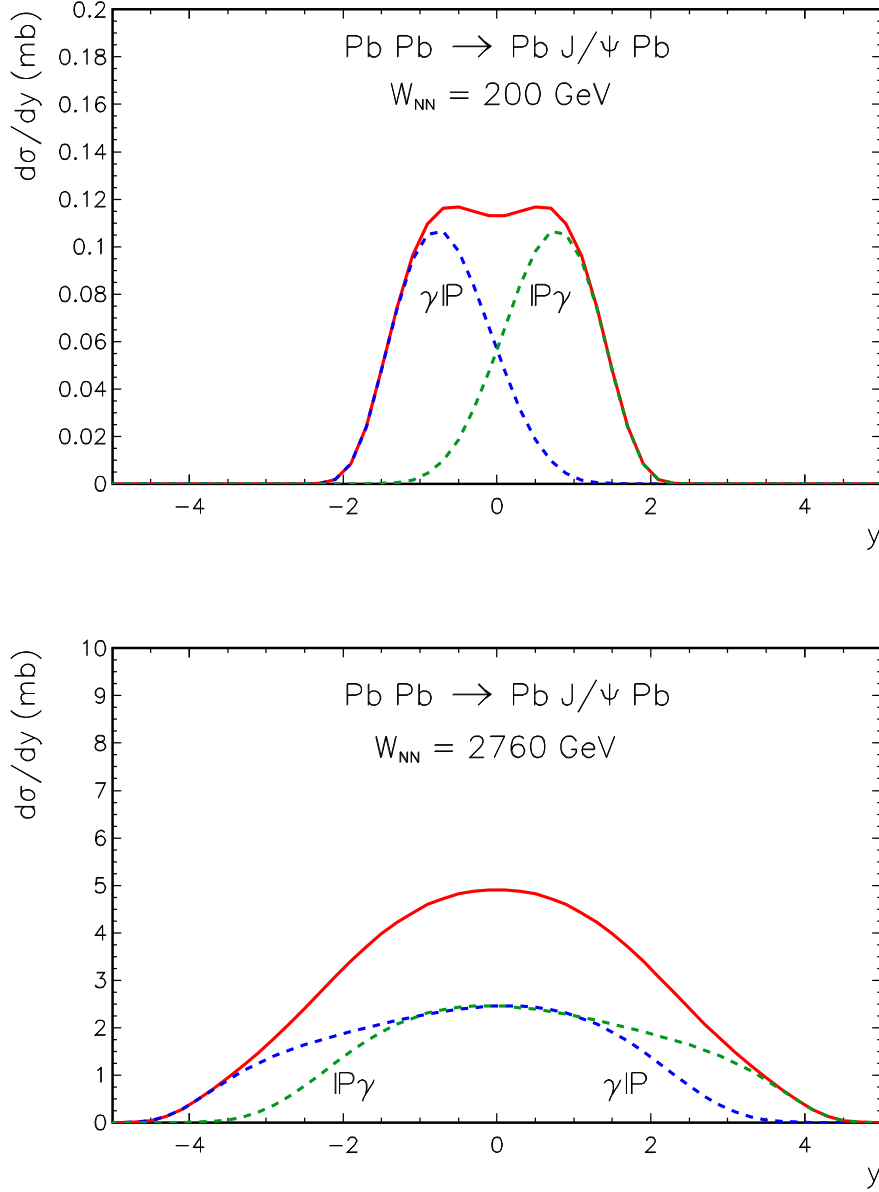


FIG. 7: Rapidity distribution of J/Ψ for symmetric collisions of lead nuclei for $W_{NN} = 200$ GeV (upper) and $W_{NN} = 2760$ GeV (lower). Individual contributions are shown separately.

is substantially bigger. In Figs. 7 - 8 we show the differential cross section in rapidity for the exclusive coherent production of J/Ψ and Υ mesons, in lead-lead collisions. The shape of the distributions strongly depends on the collision energy. The distributions in

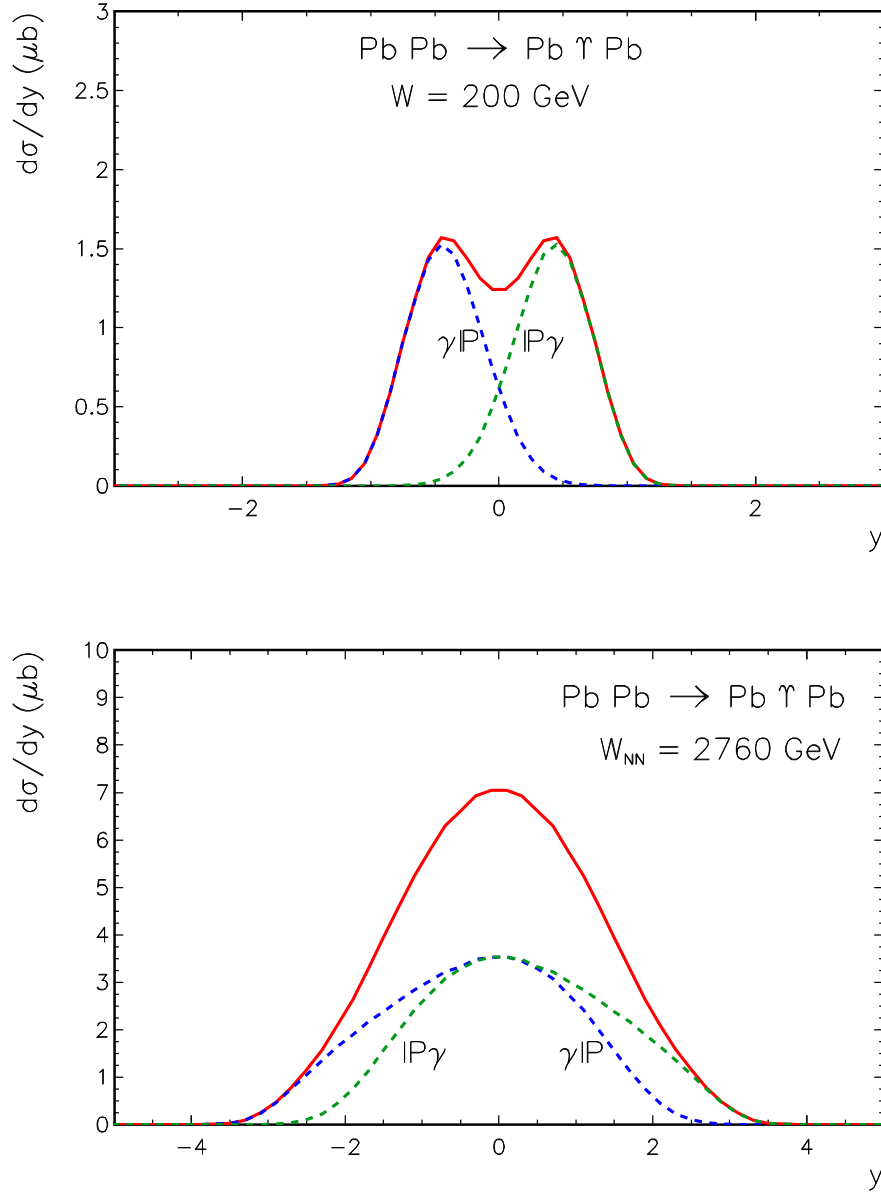


FIG. 8: Rapidity distribution of Υ for symmetric collisions of lead nuclei for $W_{NN} = 200$ GeV (upper) and $W_{NN} = 2760$ GeV (lower). Individual contributions are shown separately.

rapidity for AA collision are much narrower than similar distributions in proton-proton collisions [7, 22]. This has its origin in the large nuclear size: the charge form factor $F(q^2)$ of the nucleus is much sharper compared to the proton's Dirac form factor $F_1(q^2)$.

The spectrum of Weizsäcker-Williams photons in a proton is considerably harder than in the nucleus, see e.g. [4].

In summary, we presented predictions for the exclusive coherent diffractive production of J/Ψ and Υ -mesons in collisions of heavy nuclei at LHC energies. Our framework takes into account not only the Glauber-type rescattering of color dipoles in the nuclear matter, but also the gluon-fusion/shadowing corrections associated with the rescattering of the $Q\bar{Q}g$ -Fock-state. The predicted rapidity distributions of mesons may be tested by the ALICE experiment at LHC.

C. Acknowledgements

W.S. would like to thank Kolya Nikolaev for numerous discussions in past years related to the subject of this work. This work was supported by the MNiSW grant DEC-2011/01/B/ST2/04535.

-
- [1] I. P. Ivanov, N. N. Nikolaev and A. A. Savin, *Phys. Part. Nucl.* **37**, 1 (2006).
 - [2] K. J. Golec-Biernat, *Acta Phys. Polon.* **B35** (2004) 3103-3114; L. McLerran, [arXiv:0812.4989 [hep-ph]]; Y. V. Kovchegov, *Nucl. Phys. A* **854**, 3 (2011).
 - [3] A. Deshpande, R. Milner, R. Venugopalan and W. Vogelsang, *Ann. Rev. Nucl. Part. Sci.* **55**, 165 (2005).
 - [4] G. Baur, K. Hencken, D. Trautmann, S. Sadovsky and Y. Kharlov, *Phys. Rept.* **364**, 359 (2002).
 - [5] T. H. Bauer, R. D. Spital, D. R. Yennie and F. M. Pipkin, *Rev. Mod. Phys.* **50**, 261 (1978) [Erratum-ibid. **51**, 407 (1979)].
 - [6] N. N. Nikolaev, *Comments Nucl. Part. Phys.* **21**, 41 (1992); B. Z. Kopeliovich, J. Nemchik, N. N. Nikolaev and B. G. Zakharov, *Phys. Lett. B* **309**, 179 (1993); J. Nemchik, N. N. Nikolaev, E. Predazzi and B. G. Zakharov, *Phys. Lett. B* **374**, 199 (1996); *Z. Phys. C* **75**, 71 (1997).
 - [7] A. Rybarska, W. Schäfer and A. Szczurek, *Phys. Lett. B* **668** 126 (2008).

- [8] N. N. Nikolaev, B. G. Zakharov, Z. Phys. **C49**, 607 (1991).
- [9] S. Chekanov *et al.* [ZEUS Collaboration], Eur. Phys. J. C **24**, 345 (2002).
- [10] A. Aktas *et al.* [H1 Collaboration], Eur. Phys. J. C **46**, 585 (2006).
- [11] J. Breitweg *et al.* [ZEUS Collaboration], Phys. Lett. B **437**, 432 (1998); S. Chekanov *et al.* [ZEUS Collaboration], Phys. Lett. B **680**, 4 (2009).
- [12] N. N. Nikolaev, W. Schäfer, G. Schwiete, Phys. Rev. **D63** 014020 (2001).
- [13] V. Lukyanov, E. Zemlyanaya and B. Slowinski, [nucl-th/0308079]; V. Lukyanov and E. Zemlyanaya J. Phys. G **26** 357 (2000).
- [14] N. N. Nikolaev, B. G. Zakharov, Z. Phys. **C64** 631 (1994).
- [15] I. Balitsky, Nucl. Phys. **B463** 99 (1996); Y. V. Kovchegov, Phys. Rev. **D60** 034008 (1999).
- [16] N. N. Nikolaev, W. Schäfer, Phys. Rev. **D74** 014023 (2006).
- [17] N. N. Nikolaev, W. Schäfer, B. G. Zakharov, V. R. Zoller, JETP Lett. **84** 537 (2007).
- [18] I. P. Ivanov and N. N. Nikolaev, Phys. Rev. D **65**, 054004 (2002).
- [19] S. Klein and J. Nystrand, Phys. Rev. C **60**, 014903 (1999).
- [20] V. P. Goncalves and M. V. T. Machado, Phys. Rev. C **84**, 011902 (2011).
- [21] V. Rebyakova, M. Strikman and M. Zhalov, Phys. Lett. B **710**, 647 (2012).
- [22] W. Schäfer and A. Szczurek, Phys. Rev. **D76**, 094014 (2007).
- [23] G. Baur and L. G. Ferreira Filho, Nucl. Phys. A **518**, 786 (1990).